# Design study of a novel regenerative pump using experimental and numerical techniques.

**Dr. F J Quail[a], Dr. M Stickland[b] , A Baumgartner[b]**

[a] *Institute of Energy and the Environment, University of Strathclyde, Glasgow, G11XW, Scotland.*
[b] *Department of Mechanical Engineering, University of Strathclyde, Glasgow, G11XJ, Scotland.*

**Abstract.** This paper presents a numerical and experimental analysis of a new regenerative pump design. The complex flow-field within regenerative pumps represents a significant challenge to previous published mathematical models. The new pump design incorporates a new axial inlet and outlet port.
The experimental and numerical results demonstrate that it is not only possible to resolve the flowfield for this pump type but also demonstrates this pump as a viable alternative to other kinetic rotodynamic machines. The use of the latest rapid manufacturing techniques have enabled the production of the complex geometry of the axial ports required for the new configuration.

**Keywords**: **CFD, regenerative pump, experimental techniques, novel rapid manufacturing**

**Nomenclature**

| | | | | |
|---|---|---|---|---|
| *A* | Cross sectional area | ($m^2$) | **Superscripts** | |
| *D* | Impeller diameter | (m) | | |
| *P* | Power | (kW) | * | Intermediate variable |
| *Q* | Volume flow rate | ($m^3/s$) | – | Mean value |
| U | Mean fluid velocity | (m/s) | | |
| ρ | Density | ($kg/ m^3$) | | |
| r | Radius | (m) | **Subscripts** | |
| H | Head | (m) | *o* | open channel |
| p | Pressure | ($kN/m^2$) | *c* | circulatory |
| N | Rotational speed | (rev/min) | *sp* | Suction port |
| g | Gravitation acceleration | ($m/s^2$) | *dp* | Discharge port |
| ω | Angular velocity | (rad/s) | *t* | tangential |
| $\alpha$ | Incidence factor | | *e* | exit |
| ζ | Ellipse angle | (rad) | *i* | inlet |
| D | Diameter | (m) | s | Solid body |
| θ | Angle measured from inlet | | 0 | Inner channel |
| $\sigma$ | Slip Factor | | 2 | Impeller tip |
| Z | Number of impeller blades | | 3 | Outer channel |
| $\varphi$ | Flow Coefficient | | | |
| $\vartheta$ | Effectiveness of circulatory flow | | | |
| $\psi$ | Head Coefficient | | | |
| K | Loss coefficient | | | |
| b | Impeller width | (m) | | |
| c | Impeller tip clearance | (m) | | |
| d | Channel width | (m) | | |
| U | Peripheral velocity | (m/s) | | |
| NPSH | Net Positive Suction Head | (m) | | |
| η | Efficiency | | | |

## 1. INTRODUCTION

Pumps are the single largest user of electricity in industry in the European Union, and of those pumps, centrifugal pumps represent some 73% of all pump types [1]. The regenerative pump like the centrifugal pump is a kinetic pump however the regenerative pump can in many applications offer a more efficient alternative [2]. There is limited published data and insufficient design guiding criteria to allow more intuitive industrial selection of this pump type, particularly to meet more stringent European pump selection criteria [3].

The existing numerical models are limited in representing the complex flow-field within the pump and require significant experimental correction. Most of the theories presented, relied on assumptions not based on detailed measurements or precise CFD modelling.

The previous published theories rely on experimental corrections that take no spanwise account of flow. To date, the most fruitful research work has come from corresponding flow visualisation studies [4-7]. This paper considers a numerical and experimental analysis of a new regenerative pump design to simulate the flowfield and match pump performance. This paper considers the performance of the new pump by comparing a revised 1D model with new experimental test results and a corresponding CFD analysis. This paper presents the use of a commercially available solver; FLUENT [8], in conjunction with new experimental testing to resolve the flowfield. The main characteristic of regenerative pumps is the ability to generate high discharge pressures at low flowrates, and ability to operate with very small NPSH, [2]. Although the pump has other advantages over centrifugal type pumps the main challenge is to understand and improve the hydraulic efficiencies, typically 35-50%. The highest ever reported efficiency for the regenerative pump of 50% [9].

The complex flow-field within the regenerative pump represents a significant challenge to existing mathematical models. Regenerative pumps are the subject of increased interest in industry as these pumps are low cost, low specific speed, compact and able to deliver high heads with stable performance characteristics with other benefits [10].

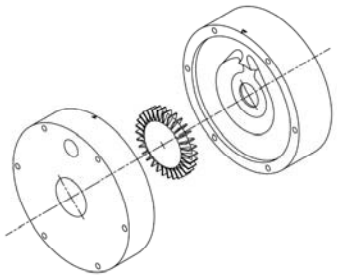

**FIGURE 1.** New Axial Flow Port Regenerative Pump Arrangement

## 2. THE REGENERATIVE PUMP

The pump uses an impeller with turbine-type blades mounted on the periphery, running in an annular channel surrounding the periphery of the impeller, Fig. 1. In the standard design, the impeller has radial teeth machined into the impeller periphery and the fluid passes through an open annular channel and circulates repeatedly through the impeller vanes, Fig. 2.

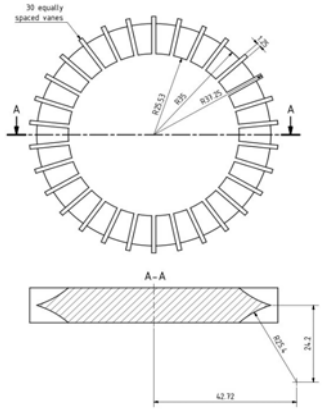


**FIGURE 2.** Regenerative Pump Radial Impeller

The regenerative pump is sometimes also referred to as a peripheral pump, turbulence pump, friction pump, turbine pump, drag pump, side channel pump, traction pump or vortex pump [10].

The suction region is separated from the discharge region by a barrier on the casing known as a 'Stripper', Fig. 3. The repeated fluid circulation during the flow process or 'multistaging', principally allows regenerative pumps to generate high heads at relatively low specific speeds. In spite of having operating characteristics that mimic a positive displacement pump (power directly proportional to head, with maximum power required at shutoff, and a steep head-capacity curve), the regenerative pump is a kinetic pump. That is, kinetic energy is imparted to the fluid by the continuous impulses given to the fluid by the rotating impeller blades. At inlet the fluid splits to both sides of the impeller and continuously circulates between the blades and the channel.

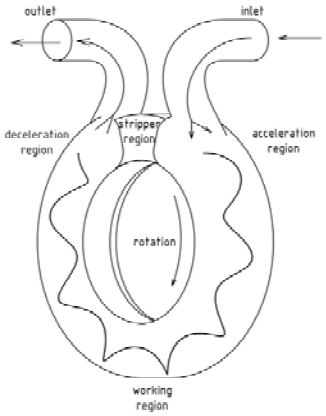


**FIGURE 3.** Regenerative Pump Helical Flow Path

When the circulation flow in the impeller and the peripheral flow in the channel unite, the momentum exchange that takes places develops a helical or corkscrew fluid motion [10]. The regenerative pump will develop significantly higher heads than a centrifugal pump with comparable impeller size [2]. The objective of the numerical approach is to predict performance over a range of running conditions that can be validated by experimental testing. Furthermore, a suitably validated CFD model provides the opportunity to demonstrate flow field representation without the significant expense of experimental flow visualisation.
The outer channel diameter for the pump is defined to 80mm. All other dimensions are due to empirically developed design criteria (section 5). The aspect ratio between channel width and channel height $AR$ and the inner channel diameter $r0$ specify the rest of the outer dimensions. This aspect ration is expressed by

$$AR = \frac{b+d}{r_3 - r_0} \qquad (1)$$

The Anderson Aspect Ratio is not applicable on regenerative pumps. In a centrifugal pump, all of the fluid leaving the impeller has to go through the throat. This aspect ratio is reasonable for centrifugal pumps because it describes an important loss mechanism over the whole range of flowrates. For regenerative pumps the varying number of circulations makes it more complicated to calculate corresponding discharge port/circulatory flow areas. A more important aspect ratio is the ratio between channel height and channel width determining how the four 90° bends in the circulatory flow path, and therefore the circulatory flow loss, correspond.

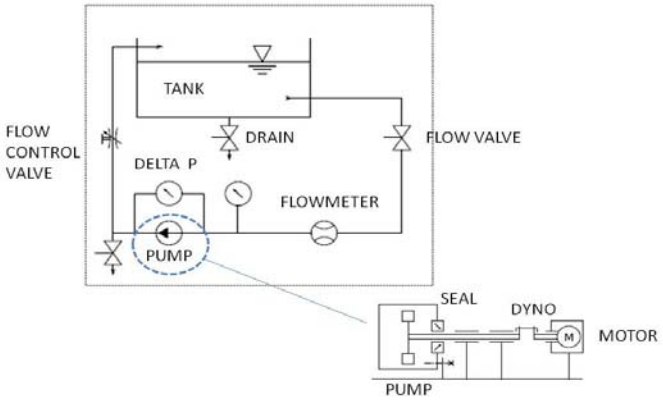


**FIGURE 4.** Regenerative Pump Rig Schematic

## 3. EXPERIMENTAL PROCEDURE

The experimental rig arrangement, Fig. 4, incorporated a reservoir tank which stored and ultimately received the working fluid, in this case water. The fluid was drawn to the pump from the tank and the fluid flow was adjusted via a flow control valve in the return line to the tank.

The fluid flowrate was measured using a Hall Effect turbine flowmeter, (0-50 l/min), situated upstream of the flow control valve and upstream of the pump. The pump itself was driven by a 3kW induction motor operating at a constant speed of 3000rpm. The motor housing was coupled to a dynamometer containing a load cell to measure strain and hence indicate input torque to be used in the pump efficiency calculations.

The test impeller had 30 blades of width 11 mm and diameter 74.5mm. The pump was of double suction shape designed with alignment of the blades to balance axial thrust, Fig. 1. In the current study a radial impeller was used with teeth `or vanes` machined into each side at its periphery. The measurements were collected using a data acquisition unit and pump characteristic head, flow and efficiency coefficients can be calculated as expressed in conventional dimensionless terms Eq. (1-3).

$$\psi = \frac{gH}{\omega^2 r_g{}^2} \qquad (2)$$

$$\varphi = \frac{Q}{\omega A_o r_g} \qquad (3)$$

$$\eta = \frac{Q\Delta p}{P} \qquad (4)$$

The dimensionless plots are used to compare pumps of different sizes and shapes.

## 4. MANUFACTURE

Until now regenerative pump port geometry have retained a fairly basic geometric configuration with simple radial inlet and outlet ports machined into the casings [11]. The purpose of this paper was to find a rapid prototyping technique that was robust enough to produce, for the first time, more complex regenerative pump inlet and outlet ports for conducting experimental tests [12]. Rapid Prototyping using `Objet Polyjet™ ,[13], (photopolymer jetting technology) techniques to build the components in thin layers (0.016mm) enabling smooth, accurate and highly detailed parts to be produced in a range of materials directly from CAD models. This enables horizontal layers of just 16-micron (0.0006"), exceptionally fine details, and ultra-thin walls down to 0.1-0.3mm typical (accuracy varies according to the geometry, part orientation and print size Fig 5.

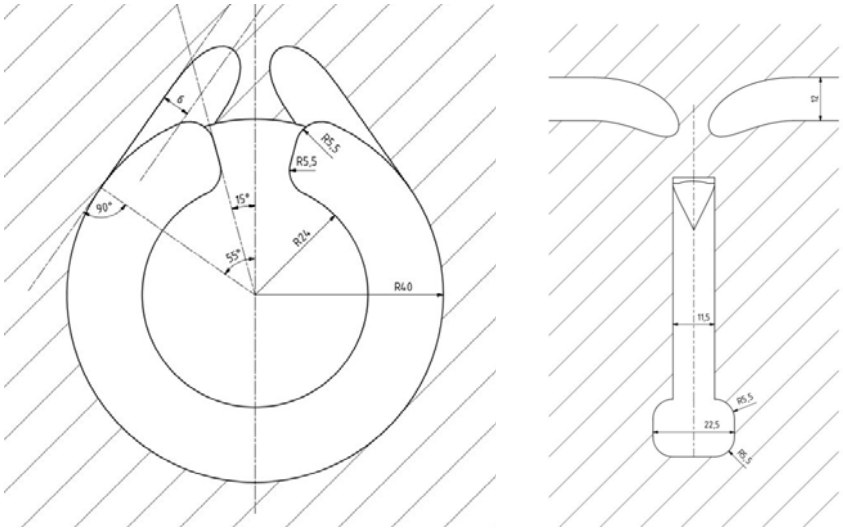


**FIGURE 5.** Casing Fluid Channel Region.

## 5. 1D MODELLING

In order that a suitable geometric configuration was developed for the pump testing a 1D model is expressed in the following manner first developed by Wilson [14]. The head of the pump is calculated from the angular momentum exchange or circulatory head rise $gH_c$ and the losses occurring in the pump. These are suction port head loss $\Delta gH_{sp}$, discharge port head loss $\Delta gH_{dp}$ and tangential head loss $\Delta gH_t$. The head rise of the pump is expressed by

$$gH = \vartheta gH_c - \Delta gH_{sp} - \Delta gH_{dp} - \Delta gH_t \tag{5}$$

$$gH_c = \frac{A_c \overline{V}_c}{Q_s}\left(\sigma U_e^2 - \alpha U_i^2\right) \tag{6}$$

The circulatory velocity depends on the friction of the circulatory flow and the sudden expansion and contraction losses when the fluid enters and exits the impeller, [15]. This equation is derived from Wilson [14] who was the first to describe the momentum exchange.

Modifying the equation for radial blade impellers leads to a simplified version of the equation for $\overline{V}_c$ which can be expressed by:

$$\overline{V}_c = \lambda\sqrt{\frac{2(1-\varphi)\left(\sigma U_e^2 - \alpha U_i^2\right) - (1-\alpha)^2 U_i^2}{K_c}} \tag{7}$$

### 5.1 EFFECTIVE CIRCULATORY FLOW.

Only the part of the fluid that enters and exits the impeller contributes to the momentum exchange. Is the center of the circulation too far away from the edge of the blade not all of the circulation transports momentum into the channel. This factor gives an approximation for this fact. However the factor only depends on the geometry, it does not account for multiple circulations. The effectiveness of circulatory flow was expressed by Yoo [16] as

$$\vartheta = 1 - \left(\frac{z_c}{b + z_c}\right)^2 \tag{8}$$

### 5.2 Loss flowrate

The true flowrate $Q_o$ in the pump deviates from the overall or desired flowrate Q. A loss flowrate $Q_l$ has to be calculates and added to the desired flowrate. A certain amount of fluid does not exit the pump after going through the pumping region but slips through the stripper. The fluid is mixed with low pressure fluid from the suction and does not contribute to the fluid power. This is called loss flowrate $Q_l$ and calculated by Wilson's [14] formula for the loss flow coefficient $\varphi_l$. It contains the loss due to flow through a series of orifices and due to the drag of the impeller. The loss flowrate equals the internal flowrate $Q_0$ at shut-off condition.

$$\varphi_l = \frac{2(h+b)\delta}{A_o}\left(\frac{r_2}{r_{g,o}} + 2C_D\sqrt{2\frac{\theta_P}{Z_{st}}\frac{\partial\psi}{\partial\theta_P}}\right) - \frac{h^2\delta}{A_o r_{g,o}} \tag{9}$$

### 5.3 Suction/discharge geometry

Previous mathematical models [16, 17] do not represent the characteristics of the new pump geometry and design. For this pump a revised suction and discharge geometry has been developed in order to grant multistaging capabilities. Its dimensions are restricted due to its complexity, Fig 5.

A non-linear equation system has to be solved for the bend radius $R_{bend}$, the flow entry point a, and the ellipse angle ζ for a given suction/discharge diameter $D_{sp/dp}$ and a safety distance $s$.

The equation system is given by:

$$\sqrt{\left(a + a\cos\zeta\right)^2 + \left(R_{bend} + R_{bend}\sin\zeta i\right)^2} - \frac{D_{sp/dp} + s}{2} = 0 \tag{10}$$

$$R_{bend}\ cos(\zeta)(R_{bend} + R_{bend}\ sin(\zeta)) - a\ sin(\zeta)(a + a\ cos(\zeta)) = 0 \qquad (11)$$

$$\frac{a}{sin\left(\frac{\pi}{2} - arcsin\left(\frac{a}{r_3}\right) - arcsin\left(\frac{d}{r_3}\right)\right)} - R_{bend} = 0 \qquad (12)$$

For the performance calculation the length of the suction and discharge ports, $l_{bend}$ and the suction/discharge cross-section, $A_{\frac{sp}{dp}}$ are needed. They can be represented as follows:

$$l_{bend} += \frac{\pi}{2R_{bend}} \qquad (13)$$

$$\vartheta_p = 2\pi - 2\arcsin\left(\frac{a}{r_3}\right) \qquad (14)$$

$$A_{\frac{sp}{dp}} = \left(\frac{D_{\frac{sp}{dp}}}{2}\right)^2 \pi \qquad (15)$$

### 5.4 Pump Flow Dimensions

The coordinates of the circulatory pivot ( $z_c$ , $r_c$ ) were calculated as a comparison between the wetted volumes. With this approach conservation of mass is maintained unlike other one dimensional models. Hereby $z_c$ is the distance from the edge of the impeller with the positive direction pointing towards the open channel and $r_c$ the distance from the pump axis. The coordinates are expressed by

$$r_c = \frac{b}{b+d}\frac{tZ}{2\pi} + \sqrt{\left(r_2 - \frac{b}{b+d}\frac{tZ}{2\pi}\right)^2 + \frac{B_u - B_b}{b+d}} \qquad (16)$$

$$z_c = \frac{B_r - B_l}{r_3^2 - r_0^2} \qquad (17)$$

### 5.5 Mean radii

The mean radii of the flow, namely inlet radius $r_i$ and outlet or exit radius $r_e$ are expressed

$$r_i = \sqrt{\frac{3}{10}\frac{4r_o^3 + 3r_o^2 r_c + 2r_o r_c^2 + r_c^3}{2r_o + r_c}} \qquad (18)$$

$$r_e = \sqrt{\frac{3r_c^5 + 10r_2^2 r_3^2 (2r_3 - 3r_c) + 15r_2^4 r_c - 8r_2^5}{10(r_3 - r_c)^2 (2r_3 + r_c)}} \qquad (19)$$

### 5.6 Slip factor for regenerative pumps

A slip factor is a measurement for the peripheral flow alignment. The difference of the circumferential velocity U to the circumferential component of the absolute velocity exiting the impeller Cu. Formally σ = Cu / U . This factor depends on the flow guidance by the impeller and would be unity for an infinite number of blades. Stodola [18], Wiesner [19] and Stanitz [20] proposed different equations to calculate the slip factor for radial centrifugal pumps $\sigma$ without knowing the absolute velocity at the vane exit.

This value is not directly applicable for regenerative pumps because of the circumferential pressure difference. The pressure difference leads to further misalignment and decreases the slip factor.
The slip factor σ was calculated with the slip factor for radial centrifugal turbomachines σ* and a term for the decrease of the slip factor because of the circumferential pressure difference. The equation is a function of the flowrate leading to a linear increase of the slip factor with increasing flowrate. Other 1D approaches, [21], on the contrary used a constant slip factor. In the current study slip was expressed by

$$\sigma = \frac{\sigma^* + \left(1-\sigma^*\right)\left(1+\frac{Q_v}{Q_s}\right)\frac{r_{g,o}}{L_c}\varphi_0}{1+\left(1-\sigma^*\right)\left(1+\frac{Q_v}{Q_s}\right)\frac{r_e}{L_c}} \tag{20}$$

### 5.7 Shock factor (incidence factor)

The shock factor $\alpha$ can be expressed as the degree of alignment between the inlet flow angle to the impeller vane angle. It depends in contrast to σ on the radius of the inlet $r_i$ and on the flow coefficient $\varphi_0$. It was evaluated as

$$\alpha = 2\frac{r_{g,o}}{r_i}\varphi_0 - \frac{r_e}{r_i}\sigma \tag{21}$$

### 5.8 The linear region factor

In order to represent the circulatory velocity with respect to the acceleration / deceleration regions a linear region factor was introduced. It describes the ratio of the linear pumping region to the full pumping region. In the theory of Wilson et al. [18] this factor is unity. This behaviour is very unlikely because it is believed that the circulatory velocity is zero at suction and discharge. To account for an acceleration and a deceleration region Badami [22] assumed a linear region factor between 0.8 and 0.95 and Song [23] assumed the linear region factor to be unity at shut-off condition which is unrealistic for reasons named above. Yoo [17] proposed a linear region factor which lead to unrealistic values for the linear region factor for the new pump geometry presented in this work. In this paper a new linear region factor is proposed.

The linear region factor consists of a constant called $\lambda^*$ and a regression factor. The constant accounts for a flow property that cannot be resolved by the one dimensional model namely the acceleration and deceleration region. The regression factor is introduced because the circulatory flow develops faster at low flowrates where the number of circulations the fluid goes through is higher. For an infinite number of circulations the regression factor would be unity. For one circulation the regression factor becomes zero indicating that there is no development. Formally the linear region factor was expressed by

$$\lambda = \lambda^* \frac{N_c - 1}{N_c} \tag{22}$$

The number of circulations is evaluated by:

$$N_c = \frac{\theta_P r_{g,o} A_o V_{c,L}}{Q L_c} \tag{23}$$

## 6 CFD MODELLING

Fluent Best Practices for Rotating Machinery, [24], recommends that for complex turbomachinery geometry, a non-conformal hybrid hexahedral / tetrahedral mesh is appropriate, where the rotation of the rotor is treated as a steady-state in a multiple reference frame model (MRF). In the case of the regenerative pump separate meshes were generated for the rotating impeller and the stationary casing Fig.6. The pump flow was then solved in local rotating reference frames where fluxes are locally transformed from one frame to another at the pump zone interfaces.

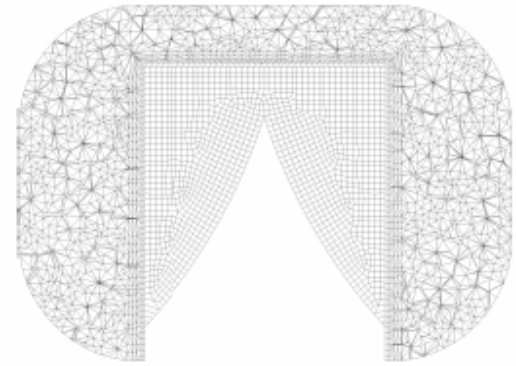

**FIGURE 6.** Impeller / Casing Fluid Region Mesh.

Most of the published data until now suffers from two fundamental problems which limit their use as a design tool. The first is the reliance on empirically derived loss factors which are not directly related to design parameters. The second defect is that previous models take no account of spanwise variation, [25]

## 7 RESULTS

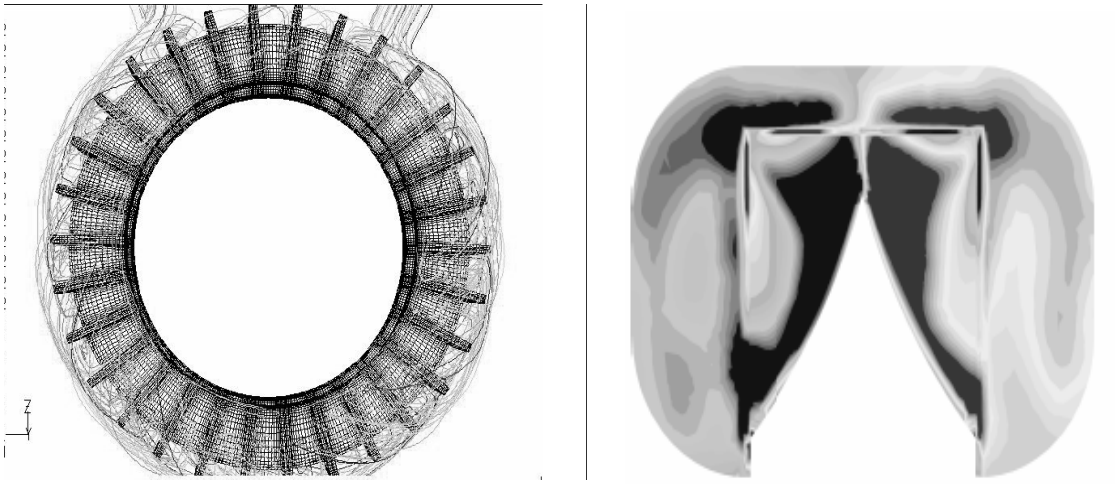

**FIGURE 7.** Regenerative Pump Helical Pathlines / Helicity Contour Plot

The numerical modelling approach demonstrates the ability to successfully capture the flow field in a manner that has not been achieved by the flow visualisation experiments, as indicated in Fig. 7. The pathlines plot indicates the helical or corkscrew motion that occurs within the pump. The helicity can be displayed in a section through the impeller and channel fluid region to depict the strong helicity gradient at the interface region between the impeller and channel region in the helicity contour plot Fig 7.

When the flow in the side channel unites with the circumferential flow in the impeller, the momentum exchange that occurs [14] is the mechanism which initiates and sustains the helical fluid flow, [10].

Experiments conducted, [4-7], used small thread probes at different points in the annular flow passage of the pump to determine the direction of the flow velocity. They were able to corroborate the helical streamlines when plotting the results. With decreasing flowrate, pump circulation is considerably increased reaching a maximum as the flow from the pump is reduced [10]. Previous work [25] that does not describe the helical flow nature instead concludes that a constant circulation rate is observed with reducing flowrate. These theories conclude that the circulation is only dependant on the resistance of the flow in the side channel and the impeller and is independent of the pressure in the working channel.

Previous work by the author indicates that in fact, local pressure variations occur across impeller vanes [10]. The static pressure varies both in the channel and the impeller, as the flow decelerates and accelerates in the pump as it makes a helical flow path through the pump.

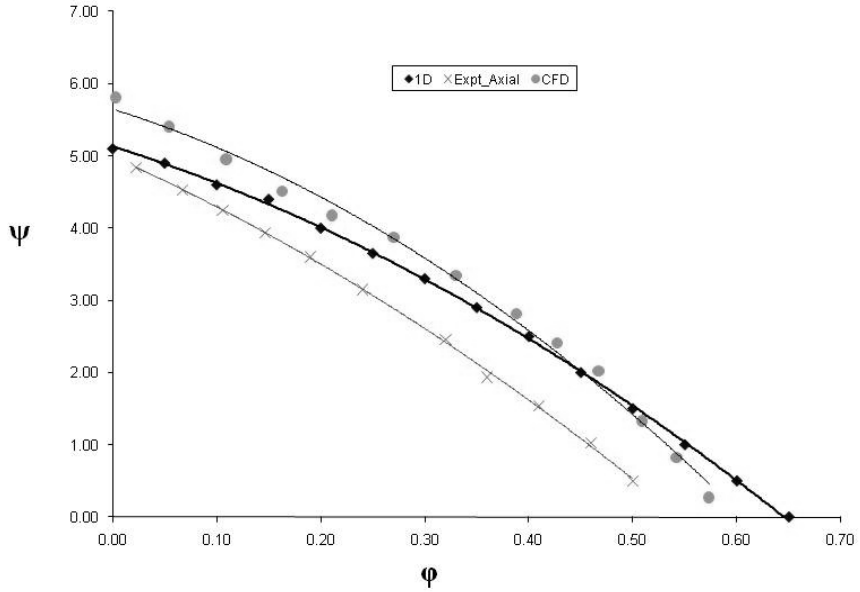


**FIGURE 8.** Regenerative Pump Helical Pathlines / Helicity Contour Plot

The CFD approach is beneficial not only in visually representing the flow physics but also in the ability to predict the performance of the pump in the model without the need for experimental correction factors as is clear in Fig 8. The reasonable concurrence between the experimental results and the CFD predictions is indicated. The axial port regenerative pump experimental results compares favorably with the 1D model developed in this current study. The new axial port regenerative pump can be much more compact than the radial flow version and will also permit multistage arrangement.

The 'multistaging' effect that allows regenerative pumps to generate high heads at relatively low speeds is not only indicated, but the potential benefit of multiple pump units arranged in sequence provides the opportunity to develop extremely high heads of pressure in very compact arrangements compared to other kinetic pump devices. When considered against centrifugal devices of similar specific speed, the efficiency of the regenerative pump can in many applications be higher, [2].

The head rise follows the established characteristic of a regenerative pump Fig 8. In the current study the experimental results and the numerical predictions indicate that the 1D modelling and CFD predications were reasonable. Indeed the flow visualisation results augment the knowledge obtained in previous studies [4-7]

Most authors have concluded that substantial efficiency and performance improvement would be attained with better understanding of the flowfield in the regenerative pump [21, 22, and 23].

Whilst the current study has indicated reasonable numerical matching (1D and CFD) to the experimental test results currently the CFD modelling techniques are being revised to consider transient analysis to capture the interaction effects particularly for the axial design where the flow geometry has high degrees of curvature and is known to be less accurate at interface boundaries [26]. In addition multistage rig testing is being conducted at present and the results will be published in the coming months.

## 8 CONCLUSIONS

There are a number of conclusions that may be drawn with regard to effectively matching the regenerative pump numerical models with the experimental data. 1D modeling results produced a reasonable representation of the performance in a regenerative pump and are currently being utilised to develop investigation for unit performance improvement. As the capabilities of CFD continue to develop, it is to be expected that the uncertainties associated with CFD prediction should also reduce. At the very least it is to be expected that there will be a continuing growth in processing power for the foreseeable future, which will reduce and perhaps remove the geometric simplifications which have to currently be made.

This work has been useful to not only benchmark current regenerative pump design, but gives confidence in the ability of CFD to capture the flow visulisation results. The 1D geometry selection presented in this paper is being developed to investigate further geometric configurations of the pump in the future. The ability of the models to establish a reasonably good representation of the pump under steady state incompressible conditions is the starting point to investigate the design modifications necessary to operate the pump in more challenging configurations. In conjunction with the numerical modellling developments there is a need for significant developments in instrumentation technology and novel approaches which enable detailed data to be acquired over large regions at higher accuracy at a reasonable cost.

## 9 REFERENCES


1. IMechE, *Energy Saving in pumps and Pumping*, Fluid Machinery Group Symposium (2007)
2. S, Mueller, *Consider regenerative pumps for low flow/low NPSH applications*. Hydrocarbon processing pg 55-57 (2004)
3. European Parliament, *Establishing a framework for the setting of ecodesign requirements for energy using products*, Directive 2005/32/EC (2005)
4. H. Engels, *Investigations of Ring pumps*, Tech Hoch Hannover. (1940)
5. J. Bartels, *Performance of a peripheral pump* -Associate Professor, Polytechnic Institute of Brooklyn (1947)
6. L. Lazo, T. Hopkins, *Theoretical and experimental analysis of a regenerative turbine pump*, Massachusetts Institute of Technology (1953).
7. G.F. Lutz, *Experimental Investigation of the pressure distribution in a regenerative turbine pump*, Massachusetts Institute of Technology (1953).
8. FLUENT version 6.3.26.: © ANSYS Inc. All Rights Reserved (2006)
9. E. Crewdson, *Water-ring self-priming pumps*. -Proceedings of the Institution of Mechanical Engineers Vol. 170 No. 13, pp. 407–415. (1956).
10. Quail, F.J., Stickland, M.T., Scanlon, T.J., 'Numerical and experimental design study of a regenerative pump'. *Current Themes in Engineering Science*, pp 165-180, American Institute of Physics, April 2010. ISBN: 978-0-7354-0766-4. Volume contains 16 invited extended papers from the World Congress on Engineering, April 2009.
11. A. Engeda, *Flow analysis and design suggestions for regenerative flow pumps*, ASME FEDSM2003-45681 (2003)
12. F.J.Quail, T.J.Scanlon, M. Stickland, *Rapid Manufacturing Technique used in the Development of a Regenerative Pump Impeller*, Proceedings of World Congress On Engineering - London (2009)
13. www.objet.com © 2009 Objet, Quadra, PolyJet, FullCure, Eden350, Eden350V are trademarks of Objet Geometries Ltd.
14. W.A.Wilson, M.A. Santalo, J.A. Oelrich, *A Theory of the fluid dynamic mechanism of regenerative pumps*, Trans. ASME Vol 77 PP1303-1316 (1955)
15. H.W. Iverson, *Performance of the Periphery Pump*, Trans ASME Vol 77 pp 19-28 (1955)
16. I. S. Yoo, M. R. Park, and M. K. Chung. Improved momentum exchange theory for incompressible regenerative turbomachines. Proc. IMechE, Part A: J. Power and Energy, 219:567 – 581, 2005.
17. J. W. Song, Abraham Engeda, and M. K. Chung. A modified theory for the flow mechanism in a regenerative flow pump. Proc. IMechE, Part A: J. Power and Energy, 217:311 – 321, 2003.
18. Stodola, A., 1945, *Steam and Gas Turbines*, McGraw-Hill,New York.
19. Wiesner F. J., 1967, "A Review of Slip Factors for Centrifugal Impellers," ASME Journal of Engineering for Power, 89, pp. 558-572
20. Stanitz, J. D., 1952, "Some Theoretical Aerodynamic Investigations of Impeller in Radial and Mixed-Flow Centrifugal Compressors," Trans ASME, 74, pp.437-476.
21. Y. Senoo, *Theoretical research on Friction Pump*, Institute of Fluid Engineering Vol 5 No1 pp 23-48 (1948)
22. M. Badami, *Theoretical and experimental analysis of traditional and new peripheral pumps*" SAE Technical Papers Series, No 971074 (1997)
23. J.W. Song, A. Engeda, M.K. Chung, *Modified theory for the flow mechanism in a regenerative flow pump*, Proceedings IMECHE, Vol 217 (2003) Power and Energy
24. FLUENT - Best Practices For Rotating Machinery (2006): © ANSYS Inc. All Rights Reserved
25. M. Raheel, A. Engeda *Systematic design approach for radial blade regenerative turbomachines* Journal for Propulsion and Power Vol. 21 (2005)
26. C.H Hirsch, *CFD Methodology and Validation for Turbomachinery Flows*, paper 4 in: AGARD-LS-195, Turbomachinery Design Using CFD. (1994)